Journal of Cellular Biochemistry 102:769–785 (2007)

Translocation of Fibroblast Growth Factor-10 and its Receptor into Nuclei of Human Urothelial Cells

Jeffrey Kosman,[1,2] Nicole Carmean,[1] Elizabeth M. Leaf,[1] Kiran Dyamenahalli,[1] and James A. Bassuk[1,2]*

[1]Program in Human Urothelial Biology, Seattle Children's Hospital Research Institute, Seattle, Washington
[2]Department of Urology, University of Washington, Seattle, Washington

Abstract Fibroblast growth factor-10 (FGF-10), a mitogen for the epithelial cells lining the lower urinary tract, has been identified inside urothelial cells, despite its acknowledged role as an extracellular signaling ligand. Recombinant (r)FGF-10 was determined by fluorescence microscopy optical sectioning to localize strongly to nuclei inside cultured urothelial cells. To clarify the possible role of a nuclear localization signal (NLS) in this translocation, a variant of rFGF-10 was constructed which lacked this sequence. rFGF-10(no NLS) was found in cytoplasm to a far greater degree than rFGF-10, identifying this motif as a possible NLS. Furthermore, this variant displayed poor or non-existent bioactivity compared to the wild-type protein in triggering mitogenesis in quiescent urothelial cells. The presence of rFGF-10(no NLS) in the nucleus suggested that additional interactions were also responsible for the nuclear accumulation of rFGF-10. The FGF-10 receptor was observed in cell nuclei regardless of the presence or concentration of exogenous rFGF-10 ligand. Co-localization studies between rFGF-10 and the FGF-10 receptor revealed a strong intracellular relationship between the two. This co-localization was seen in nuclei for both rFGF-10 and for rFGF-10(no NLS), although the correlation was weaker for rFGF-10(no NLS). These data show that an NLS-like motif of rFGF-10 is a partial determinant of its intracellular distribution and is necessary for its mitogenic activity. These advancements in the understanding of the activity of FGF-10 present an opportunity to engineer the growth factor as a therapeutic agent for the healing of damaged urothelial tissue. J. Cell. Biochem. 102: 769–785, 2007.

Key words: fibroblast growth factor-10; nuclear localization signal; FGF-10 receptor; mitogenesis

The transitional epithelial lining of the lower urinary tract, the urothelium, is exposed to an environment that constantly fluctuates in pressure, osmotic strength, and toxin concentrations. Yet the urothelium proves remarkably durable in the face of these challenges and displays one of the slowest cell turnover rates among all mammalian epithelia [Hainau and Dombernowsky, 1974; Marceau, 1990]. Inevitably, whether due to turnover, trauma, or pathogenic invasion, the urothelium must regenerate, repair itself, and reconstitute an impermeable barrier. In these cases, the cells of the urothelium are able to shed their characteristic quiescence and proliferate quickly [Hicks, 1975; Stewart, 1986], spurred by growth factors including members of the fibroblast growth factor (FGF) family [Rebel et al., 1994; Bagai et al., 2002] and epidermal growth factor (EGF) [Freeman et al., 1997; Varley et al., 2004]. Control over the proliferation of the urothelium, which may be possible by the manipulation or administration of these growth factors, would aid the clinician in the management of urethral trauma and cystitis.

While there are now 23 members of the FGF superfamily [Nishimura et al., 2000], only a few have been shown to play significant roles in urothelial development and repair. One of these, fibroblast growth factor-10 (FGF-10) has been shown in knockout mice to be a potent mitogen for the proliferation of urothelial cells [Bagai et al., 2002]. Additionally, FGF-10-null mice exhibit hypospadias [Yucel et al., 2004] and are deficient in limb bud formation and

Grant sponsor: NIH; Grant number: DK062251.

*Correspondence to: James A. Bassuk, Program in Human Urothelial Biology, Seattle Children's Hospital Research Institute, 4800 Sand Point Way NE, Mailstop A8938, Seattle, WA 98105.
E-mail: james.bassuk@seattlechildrens.org

Received 21 December 2006; Accepted 12 February 2007
DOI 10.1002/jcb.21330

pulmonary branching morphogenesis [Min et al., 1998]. Both FGF-10 and its analog FGF-7 are paracrine signaling mediators, synthesized and secreted in the lower urinary tract exclusively by mesenchymal fibroblasts underlying the urothelium [Zhang et al., 2006]. The protein traverses the basal lamina and interacts with the surface of urothelial cells, which express the FGF-10 receptor [Zhang et al., 2006]. Four types of FGF receptors (FGFR1–4) have been identified, each with multiple isoforms that determine its ligand-binding specificity [Yeh et al., 2003]. Unlike most FGFs, which interact promiscuously with multiple FGFRs, FGF-10 binds to a single isoform of FGFR2, termed isoform 2 (FGF-10 receptor), which is translated from the mRNA splice variant denoted FGFR2IIIb [Igarashi et al., 1998; Lu et al., 1999]. This isoform is a 92 kDa tyrosine kinase transmembrane receptor [Dell and Williams, 1992] which is expressed in the urothelial layers, yet is absent from the underlying fibroblasts [Zhang et al., 2006]. Thus, FGF-10 and the FGF-10 receptor constitute a paracrine signaling system designed to stimulate urothelial cell proliferation when necessary.

Until recently, the modus operandi of FGF-10 in the lower urinary tract was viewed as straightforward. As with other FGFs, FGF-10 was thought to be secreted from source cells (i.e., fibroblasts), transported, and bound by a tyrosine kinase transmembrane receptor on target cells (i.e., urothelial cells), triggering an intracellular signaling cascade. However, other members of the FGF family have now been identified inside the nuclei of target cells. FGF-2 possesses a nuclear localization signal (NLS) [Quarto et al., 1991] and accumulates in the nuclei of astrocytes [Stachowiak et al., 1997], Schwann cells [Claus et al., 2003], and Swiss 3T3 cells [Reilly and Maher, 2001]. FGF-1 also possesses an NLS that permits such translocation. Interestingly, the mitogenic properties of FGF-1 were destroyed when its NLS was removed, but restored when a substitute NLS was inserted [Lin et al., 1996]. FGF-2 and FGF-3 have even been shown to possess multiple NLSs [Kiefer and Dickson, 1995; Sheng et al., 2004]. Similarly, recombinant (r)FGF-10 has been found in the nuclei of cultured urothelial cells, whose only source of this polypeptide was exogenous protein added to cell medium [Bagai et al., 2002]. It is therefore possible that FGF-10 encodes one or more functional NLSs which may enable additional translocation and signaling capabilities.

Proteins proceed into the nucleus through nuclear pores in one of two ways: passive diffusion or active transport. Passive diffusion is associated with small molecules; nuclear pores block the diffusion of macromolecules larger than 40–45 kDa [Silver, 1991]. Small proteins may diffuse into the nucleus according to their concentration gradient, while larger proteins rely upon docking with a family of proteins named importins, which are recognized and allowed entry by the nuclear pore complex. The requisite interface between protein and importin occurs at the NLS, a sequence of basic residues that permits the nuclear transport of large proteins [Truant et al., 1998]. An NLS is not a specific sequence of residues, but rather a cluster of basic residues in space that may be recognized by the importin. A "classic" NLS is a series of basic residues contiguous in the primary sequence of a protein. Although strict rules are difficult to formulate, an NLS is generally effective if at least four out of a given six residues are basic [Boulikas, 1993]. Consecutive basic residues contribute strongly to an NLS signal. However, a "bipartite" NLS sequence may be an equally effective motif. In this version, possessed by FGF-3 [Kiefer et al., 1994], the basic residues are fewer in number and are separated by a stretch of 10–11 residues [Dingwall and Laskey, 1991; Robbins et al., 1991]. It is suggested that these separate basic residue stretches are in fact located close to each other in space in the tertiary structure of the protein, forming a positively charged patch on the protein surface that is accessible to the importin [Picard and Yamamoto, 1987]. An NLS may be appended or inserted into many non-nuclear proteins, causing them to localize to the nucleus [Kalderon et al., 1984b]. Still, the presence of an NLS is not quite sufficient to guarantee nuclear import; the NLS must also be accessible to the importin, for an NLS buried in the interior of a protein will have no impact on nuclear localization [Boulikas, 1993].

The following experiments were intended to address the logical questions: (a) does FGF-10 encode an NLS, (b) if so, how does FGF-10 localize to urothelial cell nuclei, and (c) what, if anything, does nuclear localization contribute to FGF-10's mitogenic activity? The answers to

these questions will provide new insight into the role of FGF-10 in the repair and maintenance of the urothelium and open new possibilities for using this protein in therapeutic intervention for lower urinary tract disorders.

MATERIALS AND METHODS

Culture of Urothelial Cells

Human urothelial cells, derived from bladder and ureteric tissue, were obtained as surgical explants under a Human Subjects Protocol approved by the Institutional Review Board at Seattle Children's Hospital. Cells were initially cultured in Primaria tissue culture flasks (Becton-Dickenson, Franklin Lakes, NJ) in Defined Keratinocyte Serum-free Medium (DKSFM) (Invitrogen, Carlsbad, CA) and then passaged onto tissue culture treated polystyrene flasks (Corning Inc., Corning, NY) in the same medium.

Electrophoresis and Western Immunoblotting

Recombinant FGF-10 and cell lysates were analyzed on either 12% NuPAGE SDS–PAGE gels (Invitrogen) or discontinuous homemade 12% (w/v) polyacrylamide gels that contained 0.1% (w/v) sodium dodecyl sulfate (SDS). Samples were brought to a final concentration of 50 mM dithiothreitol (DTT) (Pierce, Rockford, IL) in loading buffer (50 mM Tris-HCl (pH 6.8), 2% (w/v) SDS, 10% (v/v) glycerol, and 0.1% (w/v) bromophenol blue) and heated for 10 min at 90°C to ensure both reduction and denaturation of the proteins. Gels were stained with GelCode Blue (Pierce) overnight. Non-reducing gels were run in a similar manner, omitting the 50 mM DTT.

Immunoblots for Western analysis were prepared by electrotransferring unstained SDS–PAGE gels to polyvinylidene fluoride (PVDF) membranes in transfer buffer (25 mM Tris-HCl (pH 8.3), 192 mM glycine, and 20% (v/v) methanol). Membranes were blocked in 1% (w/v) Casein Hammerstein (USB Corporation, Cleveland, OH) and washed in Tris-buffered saline containing 10 mM Tris-HCl (pH 7.4), 150 mM NaCl, and 0.05% (v/v) Tween-20. Protein samples were detected using 0.288 μg/ml monoclonal mouse IgG specific to C-terminal His_{6x} (Invitrogen) coupled to horseradish peroxidase. Visualization was accomplished through enhanced chemiluminescence (ECL) (GE Healthcare, Piscataway, NJ).

Construction of Plasmid Encoding rFGF-10(no NLS)

The putative NLS of FGF-10 was identified by scanning the primary sequence of FGF-10 for regions that conformed to the generalized rules for a consensus NLS. Several codons in the putative wild-type FGF-10 NLS were altered to disrupt crucial recognition elements, effectively destroying the NLS. A pET-21d plasmid (Novagen, Madison, WI) encoding an ampicillin resistance gene and the sequence of wild-type secreted human FGF-10, termed pFGF-10wt, was used as a template [Bagai et al., 2002]. Selected codons were mutated using site-directed mutagenesis (Quik-Change, Stratagene, La Jolla, CA). The following primer pair was used to generate the plasmid encoding the rFGF-10(no NLS) mutant: 5′-GCCATGAACA**C**GA**C**-CGGTA**C**ACTCTATGGCTC-3′ and 5′-GAGCC-ATAGAGT**G**TACC**G**TC**G**TGTTCATGGC-3′. Emboldened bases effected a change in amino acid sequence; underlined bases created the silent restriction site for *Age*I. Oligonucleotide primers were synthesized and cartridge purified by Sigma Genosys (The Woodlands, TX). PCR amplification of these plasmids was performed using Hotstart *Pfu* turbo (Qiagen Inc., Chatsworth, CA) and the following cycling method: 95°C for 30 s; then 18 cycles of 95°C for 30 s, 50°C for 60 s, 60°C for 20 s, and 68°C for 420 s; then an extension step of 68°C for 420 s; then cooling at 4°C indefinitely. The sequence of the entire FGF-10 cDNA insert in the resulting plasmids was verified using T7 promoter and terminator primers in the dideoxy sequencing method on an Applied Biosystems ABI3730XL DNA sequencer at the Department of Biochemistry DNA Sequencing Facilityat the University of Washington, Seattle.Sequenced plasmids that exhibited the proper coding insert were transformed into BL21(DE3) *E. coli* (Novagen), and the resultant colonies were selected on Luria-Bertani (LB) agar plates containing 50 μg/ml carbenicillin (Novagen). A single colony was picked, grown in a culture tube containing LB medium and 50 μg/ml carbenicillin, aliquotted, and frozen at −80°C in an LB solution containing 20% (v/v) glycerol for later use in protein expression. Frozen stocks were later rechecked for correct restriction enzyme digestion patterns and protein expression patterns.

Expression and Purification of rFGF-10 and rFGF-10(no NLS)

Frozen stocks of BL21(DE3) *E. coli* containing pET-21d plasmids encoding either rFGF-10 or rFGF-10(no NLS) were thawed and streaked on LB agar plates containing 50 μg/ml carbenicillin. Following overnight incubation at 37°C, a single colony was chosen to inoculate into 100 ml starter culture of LB medium containing 50 μg/ml carbenicillin. This starter culture was shaken at 37°C until an OD_{600} of 0.6–0.8 was achieved, then was stored overnight at 4°C. On the following day, the starter culture was pelleted at 4°C and resuspended in 10 ml fresh LB. The cell suspension was mixed into a total of 8 L LB medium in a New Brunswick Scientific Bio-Flo 110 fermentor (New Brunswick, NJ). The LB medium used during fermentation was made with peptone derived from meat, not milk, to avoid a possible contaminating source of lactose during protein expression. Glucose was also added to the fermentation medium at 0.2% (w/v) to minimize premature protein expression via the *lac* promoter. Alternately, PSI medium was used in fermentation, which contains LB medium augmented with 4 mM $MgSO_4$ and 10 mM KCl [Luo et al., 2004] for higher yields. The fermentor was run at 37°C at pH 7.0 with automatic pH adjustment to within ± 0.1, aeration at 10 L/min, and stirring automatically regulated to maintain dissolved oxygen in the medium at 30% of a fully aerated solution. The OD_{600} of the culture was monitored twice an hour until it reached 0.6–0.8, indicating that the cells were in mid-log exponential growth phase. The culture was induced by the addition of isopropyl-β-D-thiogalactopyranoside (IPTG, Research Products International Corp., Mount Prospect, IL) to a final concentration of 1 mM. Recombinant FGF-10, under the control of the *lac* repressor on the pET21d plasmid, was expressed for 2 h, after which the cells were pelleted at 5,000*g*, washed with a Tris salt buffer (10 mM Tris-HCl (pH 8.0), 100 mM NaCl, 1 mM EDTA), and stored at −20°C. Hourly samples were withdrawn from the culture during the fermentation for analysis on an SDS–PAGE gel.

rFGF-10 and rFGF-10(no NLS) were purified in a native state from frozen fermentation pellets as previously described [Bagai et al., 2002]. Briefly, cells were solubilized with 5 ml Bug Buster/g cell paste (Novagen) in the presence of 1 μl/ml benzonase (Novagen) and 1 tablet protease inhibitors/50 ml (COMPLETE protease inhibitor cocktail tablets, EDTA-free, Roche, Indianapolis, IN). The cell lysate was centrifuged at 16,000*g* for 30 min, and the clarified supernatant, containing soluble proteins and 10 mM imidazole, was run over a nickel-chelate nitrilotriacetic acid (Ni-NTA, Qiagen) column controlled by an AKTA purifier (GE Healthcare). Recombinant proteins bound to this column through their engineered His_{6x} C-terminal tail, a construct that has been shown not to interfere with heparin binding or mitogenic activity of rFGF-10 [Bagai et al., 2002]. The proteins were eluted in a phosphate buffer (0.5 M NaCl, 0.1 M sodium phosphate, 0.05 M Tris-HCl) by a pH gradient ranging from 8.0 to 4.5. Fractions were analyzed on 12% SDS–PAGE gels to assess the extent of contaminating proteins, and fractions containing rFGF-10 were pooled, dialyzed versus three changes of 0.1 M sodium phosphate (pH 7.0), 0.15 M NaCl, and 5 μg/ml heparin (Sigma, St. Louis, MO), filtered, and frozen. All stocks of recombinant FGF-10 were brought to 5 μg/ml heparin to ensure the stability of the stored protein. A typical preparation of protein contained 0.09 ng lipopolysaccharide (LPS)/μg protein (Limulus Amebocyte Lysate QCL-1000 Endotoxin Assay Kit, Cambrex BioScience Inc., Walkersville, MD). Such low levels of endotoxin have been shown in our laboratory not to influence urothelial cell metabolism.

Fluorescence Spectroscopy

The tertiary structure of rFGF-10(no NLS) was compared to rFGF-10 using the intrinsic fluorescence emission spectra of the two tryptophan residues in the primary structure. Proteins were dialyzed into a solution containing 1X Hank's balanced salt solution (HBSS, Invitrogen) and 10 mM HEPES (pH 7.4) (Invitrogen), filtered, diluted to 0.025 mg/ml (rFGF-10(no NLS)) or 0.05 mg/ml (rFGF-10), and loaded into a 1 cm quartz cuvette. Fluorescence spectra were collected on a Perkin-Elmer LS50B Luminescence Spectrometer using the following parameters: proteins were excited at 280 nm; scanned from 300 to 450 nm at a scan speed of 200 nm/min; five accumulations were averaged; the excitation slit width was 6 nm; and the emission slit width was 7 nm. The spectrum of a buffer blank was subtracted from all protein scans.

DNA Synthesis Assay

Primary cultures of urothelial cells were seeded at 2,000 cells/well in 96-well tissue culture plates (Costar, Corning, NY) and fed DKSFM containing the manufacturer's growth supplement (GS) (Invitrogen). Cells were incubated for at least 24 h at 37°C and 5% CO_2 to allow time to attach and resume normal metabolism, then were washed twice with DKSFM-GS, a medium from which the GS had been omitted. Cells were then fed DKSFM with or without GS and with or without 1 μM PD153035 (Roche), a potent epidermal growth factor receptor (EGFR) inhibitor. PD153035 blocks the autophosphorylation of EGFR, preventing any downstream signaling from this receptor [Fry et al., 1994]. Two days after addition of PD153035, medium was aspirated from wells, and cells were fed DKSFM that contained 5 μg/ml heparin (Sigma) with or without GS, with or without PD153035, and with or without rFGF-10. Cultures were no more than 50% confluent at this time. After cells were exposed to rFGF-10 for 42 h, 5-bromo-2′-deoxyuridine (BrdU) (Roche) was added to a final concentration of 10 μM. BrdU is an analog of thymidine and was used to facilitate the colorimetric detection of new DNA synthesis. Cells were exposed to BrdU for an additional 2 h, fixed for 0.5 h, and incubated for 1.5 h with a monoclonal mouse anti-BrdU antibody conjugated to peroxidase (Cell Proliferation ELISA, BrdU, Roche). Tetramethyl-benzidine (Roche) was added to each well as a substrate for peroxidase, producing a colored product that was measured by a Bio-Tek Powerwave XS plate reader. Relative DNA synthesis corresponded to the A_{370} for each well. The statistical significance of these results was calculated using two-tailed linear regression, with the independent variable defined as base 10 logarithm of dose of growth factor.

Immuno-Fluorescence Microscopy

Cells were prepared for immuno-fluorescence microscopy as previously described [Zhang et al., 2006]. Urothelial cells were grown on 0.17 mm thick #1.5 coverslips (SecureSlips, Grace Biolabs, Bend, OR) in DKSFM + GS. Near confluency, cells were fed DKSFM + GS with 5 μg/ml heparin (Sigma) and exposed for 16–24 h to various concentrations of rFGF-10. Fixation was accomplished with 4% paraformaldehyde (Electron Microscopy Sciences, Ft. Washington, PA) in PBS (pH 7.4) (Sigma) for 15 min. Cells were then washed thrice with PBS and permeabilized for another 15 min with 0.1% (v/v) Triton X-100 (Sigma) in PBS. Following three more washes in PBS, cells were blocked for 1 h with a 5% (v/v) normal goat or rabbit serum (Electron Microscopy Sciences) in PBS, depending upon the species origin of the secondary antibody. The primary antibody specific for the immunogen of interest was incubated with the cells for 1.5 h at room temperature or overnight at 4°C. The coverslips were washed three times with PBS containing 0.1% Tween-20 (PBS-T) (Sigma), then incubated for 1 h at room temperature with fluorescently labeled secondary antibody in PBS-T. Unbound antibodies were removed with three more washes of PBS-T. In some experiments, DNA was stained for 0.5 h with 200 nM 4′,6-diamidino-2-phenylindole (DAPI) (Molecular Probes, Eugene, OR) in PBS. The fixed and stained cells were mounted using ProLong Gold anti-fade mounting medium (Molecular Probes) and sealed with another #1.5 coverslip. The antibodies used were 1.7 μg/ml mouse monoclonal IgG_{2B} anti human FGF-10 (R & D Systems, Minneapolis, MN), 20 μg/ml mouse monoclonal IgG_1 anti FGFR2IIIb (R & D Systems), 1.9 μg/ml goat anti-mouse IgG_{2B} conjugated to Cy2 fluor (Jackson ImmunoResearch Laboratories, Inc., West Grove, PA), 15 μg/ml goat anti-mouse IgG_1 conjugated to Cy5 fluor (Jackson ImmunoResearch Laboratories, Inc.) and 3.75 μg/ml goat anti-mouse IgG conjugated to Cy2 fluor (Jackson ImmunoResearch Laboratories, Inc.). The anti-FGF-10 receptor antibody is specific for isoform 2, although there is some slight cross-reactivity with the translated product of the FGFR2IIIc splice variant, a splice variant which is not expressed in urothelial cells (Zhang, D. and Bassuk, J. A., unpublished observations). All antibodies were used at concentrations that avoided giving rise to artifacts or cross-reactivity (data not shown).

Images were collected on a DMI6000B inverted fluorescence microscope (Leica Microsystems, Bannockburn, IL) using a 40X correction collar objective (NA = 0.60), or a 63X oil immersion planapochromatic objective (NA = 1.32). Pictures were taken by either a Leica DC500 or DFC350 digital camera (1,300 × 1,030 and 1,392 × 1,040 pixel resolution, respectively). Mounted cells were optically

sectioned by collecting a stack of images varying in focal plane by 0.3 μm in the vertical dimension. The automated collection of these multichannel datasets was coordinated by ImagePro v5.0 software (Media Cybernetics, Silver Springs, MD). Out-of-focus light and haze were removed from each image in the stack by deconvolution algorithms in AutoDeblur v9.3 software (AutoQuant, Troy, NY), rendering the stack into a collated dataset of 0.3 μm thick optical slices. Exposure times were held constant for comparable images, and adjustments to each image, such as in contrast and cropping, were performed strictly in parallel between comparable datasets. Co-localization images, Pearson's co-localization coefficients (R_p), and Manders' co-localization coefficients (M) were generated by ImageJ software v1.34 (NIH freeware, http://rsb.info.nih.gov/ij). R_p calculates an overall co-localization correlation for two channels at all pixels having intensity above background. High scores (positive numbers up to 1) indicate mutual co-localization, and low scores (negative numbers down to −1) indicate mutual exclusion. M calculates the fraction of pixels with signal from one channel that coincides with pixels with signal from a second channel. High scores approaching 100% indicate strong co-localization of the first channel with the second, and low scores approaching 0% indicate no relationship [Manders et al., 1992]. Co-localization was defined as signals within the pixel resolution of 0.1 μm/pixel. Nuclei were defined as the entire area within the periphery described by DAPI signal.

RESULTS

Design of rFGF-10(no NLS)

The primary sequence of secreted human FGF-10 was analyzed to identify any potential NLS using two algorithms: PSORT II [Nakai and Horton, 1999] and PROSITE [Cokol et al., 2000]. These two programs take primary sequences of proteins and compare them to sequences of known nuclear proteins. The consensus NLS rules of Boulikas [1993] were also considered. Overall, FGF-10 is a basic protein with a pI of 9.94, and there are several short stretches of basic residues that are potential candidates for an NLS. Neither algorithm predicted a strong NLS for FGF-10, yet both identified FGF-10 as a potential nuclear protein based on its high content of basic residues. A more useful indicator of the FGF-10 NLS was its sequence similarity to another member of the FGF family, FGF-1, which possesses a known NLS [Zhan et al., 1992; Lin et al., 1996]. The FGF-1 NLS, KKPKL, is nearly identical to a basic stretch in the C-terminal half of FGF-10, KKGKL (Fig. 1B). Furthermore, the same motif, KKPKL, is found in heparin-binding growth factor 1, where it has also been identified as an NLS [Imamura et al., 1992]. In the co-crystal of FGF-10 with its receptor, this motif is located on a loop on the surface of the protein, away from the interface between receptor and ligand [Yeh et al., 2003], making it an attractive candidate for an NLS (Fig. 1A). This stretch is short enough to be overlooked by algorithms searching for strong NLS motifs, but effective enough to fulfill the most important criteria in identifying an NLS. The borderline strength of this NLS may also help explain how FGF-10 may be both secreted and transported to the nucleus.

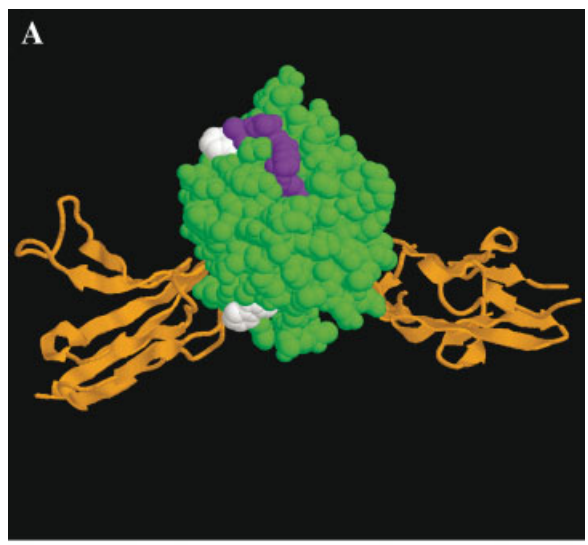

B

rFGF-10	residues 96-102:	M N **K K** G **K** L
rFGF-10(no NLS)	residues 96-102:	M N **T T** G **T** L
FGF-1	residues 21-27:	N Y **K K** P **K** L

Fig. 1. Location and mutation of FGF-10 NLS. **A**: Putative FGF-10 NLS (purple) is located on an exposed face of FGF-10 (green) in this co-crystal structure with the FGF-10 receptor (orange). W131 (white) is contiguous to the NLS. The other Trp, W41 (white), is on the opposite face. This model was constructed from atomic coordinates available in the Molecular Modeling Database (http://www.ncbi.nlm.nih.gov/Structure/MMDB/mmdb.shtml) under MMDB # 1NUN [Yeh et al., 2003] and was assembled in RasMol. Residue numbering based on mature, secreted sequence. **B**: Amino acid sequence of the putative FGF-10 NLS with mutated residues in boldface, aligned with the FGF-1 NLS.

In order to test the hypothesis that FGF-10 encodes an NLS, the key recognition elements of the putative NLS were replaced with residues that eliminated the nuclear targeting sequence. Using site-directed mutagenesis, the positively charged residues K98, K99, and K101 were replaced with electrically neutral threonines (T). A swap of negatively charged residues for positively charged ones would have certainly also eliminated any vestige of an NLS, but may also have had unforeseen consequences for the expression or folding of the polypeptide. Therefore, threonines were chosen to mimic the bulk of the lengthy lysines, and also to maintain the hydrophilic character of this region. Moreover, threonine has already been shown to disrupt the function of the NLS in other proteins when substituted for a positively charged residue [Kalderon et al., 1984a]. The key residues in the heparin-binding site of FGF-10 (residues 100–123) were not affected by these changes.

Construction, Expression, and Purification of rFGF-10 and rFGF-10(no NLS)

The construction of the pET21d-FGF10 plasmid encoding wild-type human FGF-10 has been described previously [Bagai et al., 2002]. This plasmid was used as a template for the construction of the rFGF-10(no NLS) mutant. Site-directed mutagenesis was used both to effectuate the desired changes in the amino acid sequence and to incorporate a silent restriction site into the rFGF-10(no NLS) cDNA insert. Mutated plasmid was generated and amplified by PCR, digested with the appropriate silent restriction enzyme endonuclease, and analyzed on a 1% agarose gel. Products displaying the predicted restriction patterns (not shown) were transformed into the XL-1 blue strain of *E. coli* (Stratagene). This plasmid was amplified and isolated from a single bacterial colony, analyzed again for the predicted restriction pattern on an agarose gel, and dideoxy sequenced along the entire length of the gene. The sequence of the mutant plasmids was 100% identical to the predicted sequence [Bagai et al., 2002]. Once certified, these plasmid stocks were either used fresh or were retransformed into *E. coli* for storage at -80°C.

rFGF-10 and rFGF-10(no NLS) were expressed from fermentation cultures of BL21(DE3) *E. coli* transformed with pET21d-FGF10 or its NLS variant as described in Materials and Methods Section. The expression of rFGF-10 in bacteria was found to partition into both insoluble and soluble forms [Bagai et al., 2002]. Only the soluble form has been well-characterized, and only this form was purified for further use in these studies. Bacterial pellets were lysed, and the clarified, soluble extract was applied to a Ni-NTA affinity column. rFGF-10 bound to the Ni-NTA resin with high affinity through its engineered C-terminal His-tag, while contaminating bacterial proteins flowed through the column [Bagai et al., 2002]. Residual contaminating proteins were further eliminated by (a) inclusion of imidazole in the loading buffer, reducing nonspecific interactions with the Ni-NTA resin, (b) washing the column with successively lower pH buffers, and (c) washing the column until the OD_{280} of eluant was <0.05. rFGF-10 was eluted from this column at pH 4.5, and fractions displaying high concentrations of FGF-10 and negligible concentrations of contaminants on an SDS–PAGE gel (not shown) were pooled. We conclude that our preparations of rFGF-10 were intact because (a) a band with the predicted molecular size of 20 kDa appeared on denaturing SDS–PAGE gels (Fig. 2A, lanes 4–10), (b) rFGF-10 and its no NLS variant were detected on Western blots with a monoclonal antibody against FGF-10 (Fig. 2B, lanes 4–10), (c) rFGF-10 and its no NLS variant bound to the nickel column, demonstrating the presence of the C-terminal His tag, and (d) previous preparations of rFGF-10 had the predicted N-terminal amino acid sequence, as determined by Edman degradation [Bagai et al., 2002]. The apparent molecular size of the recombinant proteins on an SDS–PAGE gel did not change upon treatment with the reducing agent DTT (Fig. 2C, lanes 2, 3, 6, and 7).

Tryptophan Fluorescence Spectroscopy of Recombinant FGF-10 Preparations

Fluorescence spectroscopy was used to examine the three-dimensional structure of rFGF-10 and rFGF-10(no NLS). The proteins were excited at 280 nm to stimulate the fluorescent emission of the only two tryptophan residues in FGF-10, W41, and W131 (Fig. 1A). The polarity of the average environment around these two residues was reflected in the wavelength of maximum fluorescence. The wavelength of maximum fluorescence was 341.5 ± 0.5 nm for rFGF-10 and 336.5 ± 0.5 nm for rFGF-10(no NLS) (Fig. 3). The shift in wavelength is likely

due to the proximity of the NLS loop to W131 in the tertiary structure of the protein (see Discussion), rather than to any destabilization caused by the mutations.

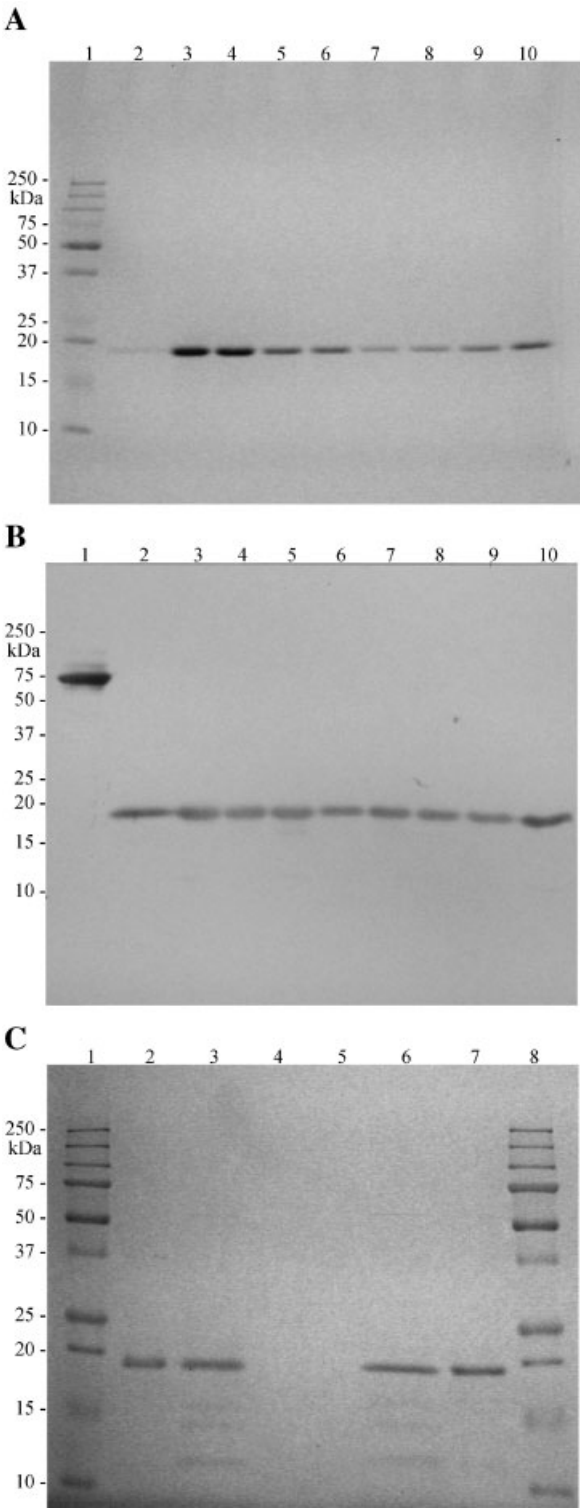

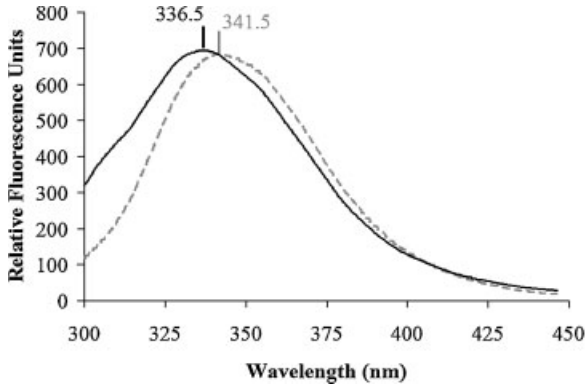

Fig. 3. Ultraviolet tryptophan fluorescence emission spectra of recombinant FGF-10 preparations. rFGF-10 and rFGF-10(no NLS) were evaluated by fluorescence spectroscopy to compare the tertiary structure of the folded proteins. Spectra were generated by exciting proteins at 280 nm and scanning emission fluorescence from 300 to 450 nm. n = 2. rFGF-10, dashed line; rFGF-10(no NLS), solid line.

Intracellular Localization of rFGF-10 and rFGF-10(no NLS)

Immunofluorescence microscopy was used to determine the extent that cultured urothelial cells would internalize exogenous rFGF-10 and rFGF-10(no NLS) from the cell culture medium, and that the proteins would accumulate in cell nuclei. Urothelial cells do not synthesize FGF-10 [Zhang et al., 2006], so all FGF-10 visualized in this experiment originated from a recombinant, exogenous source. In order to further clarify the intracellular localization of the proteins, the cells were visualized as a series of images focused along the vertical (z) plane. This series was deconvolved with an algorithm designed to eliminate out-of-focus signal, rendering a series of optical slices representing a cross-section through the cells. Shown in Figure 4 are slices through the middle of the nuclei of cells incubated with recombinant

Fig. 2. Isolation of rFGF-10 and rFGF-10(no NLS). **A**: Coomassie-stained 12% SDS–PAGE gel showing elution fractions from the Ni-NTA column in **lanes 4–10**. **Lane 1**, molecular weight markers (MWM); **lanes 2** and **3** contain recombinant protein standards. **B**: Western blot showing elution fractions from the Ni-NTA column in **lanes 4–10**. rFGF-10 was visualized with a mouse anti-His_{6x} antibody coupled to peroxidase. MWM (**lane 1**) contain a known His-tagged protein at 75 kDa. **Lanes 2** and **3** contain recombinant rFGF-10 protein standards. **C**: Coomassie-stained 12% SDS–PAGE gel showing isolated fractions of rFGF-10 (**lanes 2** and **7**) and rFGF-10(no NLS) (**lanes 3** and **6**) prepared with (**lanes 6** and **7**) and without (**lanes 2** and **3**) 50 mM DTT. **Lanes 4** and **5** are blank.

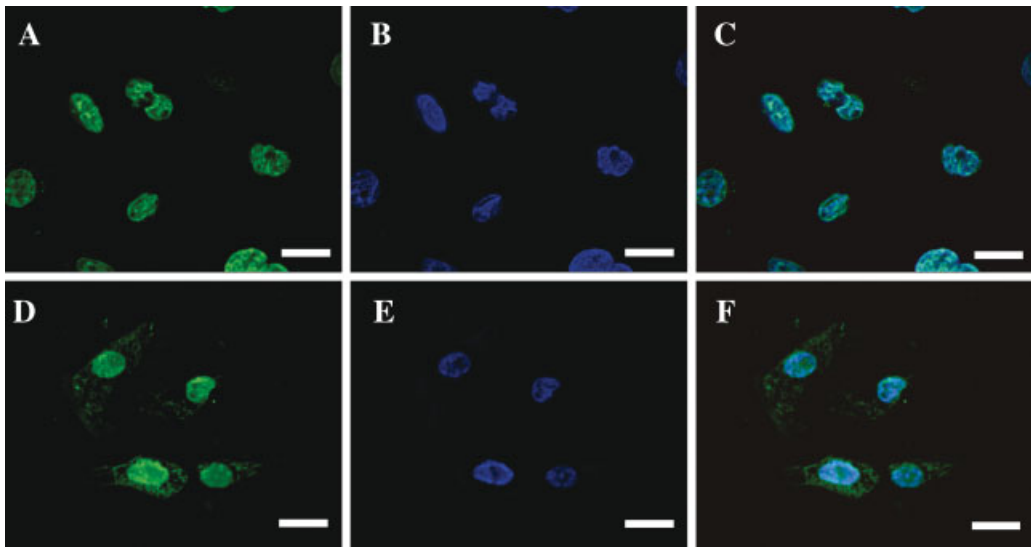

Fig. 4. Intracellular localization of rFGF-10 and rFGF-10(no NLS). Shown are optical slices of cultured urothelial cells stained for cell nuclei (blue) and rFGF-10 or rFGF-10(no NLS) (green). Cells in **panels A–B** were exposed to 10 μg/ml rFGF-10 for 24 h; those in **panels D–E** were exposed to 10 μg/ml rFGF-10(no NLS) for the same amount of time. Recombinant FGF-10 proteins (**panels A** and **D**) were detected by a mouse monoclonal primary antibody, followed by a goat anti-mouse secondary antibody coupled to the Cy2 fluor. Cell nuclei(**panels B** and **E**) were stained blue with the DNA stain DAPI. **Panels C** and **F** show the overlay of the two preceding panels. Pairs of images (**A** and **D**, **B** and **E**) were taken with equivalent acquisition parameters and contrast-adjusted in parallel. Size bars = 20 μm.

proteins. Nuclear boundaries were clearly delineated by the blue DAPI stain in these slices (Fig. 4B,E) and signals originating from either above or below the slices were removed by deconvolution. rFGF-10 immunoreactive signals were found only in cross-sections through cell nuclei (data not shown).

Urothelial cells were clearly able to take up rFGF-10 from cell culture medium (Fig. 4A). The overlay of the rFGF-10 and DAPI signals (Fig. 4C) aligned perfectly, revealing a strong translocation of rFGF-10 to cell nuclei. While rFGF-10 was presumed to have an NLS, it was interesting that the protein was found predominantly inside nuclei, for the protein on its own is small enough to diffuse through the nuclear pores and throughout the cell. Although rFGF-10 was observed in the cytoplasm to only a minor extent, FGF-10 has been observed in the cytoplasm of urothelial cells in vivo [Zhang et al., 2006], and such transport would be necessary for it to reach the nuclei.

Urothelial cells were also observed to internalize rFGF-10(no NLS) from the cell culture medium (Fig. 4D). Qualitatively, the net amount of protein internalized did not appear to differ greatly between the wild-type protein and its mutated version. Both proteins were observed to be present in cell nuclei, as shown by the overlays in Figure 4C,F. The presence of rFGF-10(no NLS) in cell nuclei was not surprising, for just as the protein is small enough to diffuse out of the nuclear pores, it is small enough to diffuse in, whether it has an NLS or not. One difference between the localization of the two FGF-10s was the presence of rFGF-10(no NLS) in the cytoplasm (Fig. 4D,F). The removal of the NLS appeared to have lessened the impetus for the protein to accumulate in the nucleus, though whether this difference is one of equilibrium or kinetics is a topic of current investigation. Regardless, the presence of rFGF-10(no NLS) in the cytoplasm is an indication that this variant achieved its intended design to disrupt the nuclear localization of rFGF-10.

Stimulation of Mitogenesis by rFGF-10 and rFGF-10(no NLS)

The ability of rFGF-10 and rFGF-10(no NLS) to stimulate DNA synthesis was further investigated in cultured urothelial cells. FGF-10 is a known mitogen for urothelial cells, and will stimulate quiescent cells to replicate their DNA [Bagai et al., 2002]. However, the FGF signaling pathway is not the only means to stimulate urothelial cell replication; the autocrine EGF

signaling pathway produces similar results [Varley et al., 2005]. Therefore, the FGF signaling pathway was isolated for study by inhibiting the EGF receptor with the highly potent and specific inhibitor PD153035 [Fry et al., 1994; Varley et al., 2004]. Cells treated with this inhibitor displayed a 59% decrease in DNA synthesis, as measured by the incorporation of BrdU into cellular DNA (Fig. 5A, compare solid black bar to bar with horizontal stripes). The FGF signaling pathway was rendered inactive by withholding the GS from the cell culture medium. These GS-starved cells reduced their DNA synthesis by 27% (Fig. 5A, compare solid black bar to bar with vertical stripes). The blockage of both of these signaling pathways was sufficient to render a sub-confluent culture of urothelial cells quiescent, as evinced by a 99% decrease in DNA synthesis (Fig. 5A, compare black bar to open bar). The results of these controls were in accord with previously published studies [Zhang et al., 2006]. The addition of rFGF-10 to the growth medium of replicating, uninhibited cells did not effect any change in the extent of DNA synthesis (Fig. 5A, compare black bar to gray bar). Thus, while rFGF-10 was sufficient to induce DNA synthesis in quiescent urothelial cells [Zhang et al., 2006], it was not able to induce further DNA synthesis in cells already engaged in this activity (Fig. 5A and data not shown).

As in previous results [Bagai et al., 2002; Zhang et al., 2006], the addition of rFGF-10 to quiescent urothelial cells induced a significant and concentration-dependent increase in DNA synthesis, even at concentrations as low as 1 ng/ml (Fig. 5B, squares). Increasing concentrations of rFGF-10 restored DNA synthesis in quiescent cells to levels comparable to that of uninhibited, proliferating cells. However, the addition of rFGF-10(no NLS) to quiescent cells did not elicit the same response as rFGF-10 ($P < 0.001$) (Fig. 5B, triangles). At low concentrations, the response was barely above baseline. In fact, even concentrations of rFGF-10(no NLS) as high as 10 μg/ml did not result in an increase in DNA synthesis equal to that observed in cells exposed to only 1 ng/ml of rFGF-10. The slope of the dose-response curve was significantly shallower for rFGF-10(no NLS) than for rFGF-10 ($P < 0.01$). Although this mutant was not entirely inactive, it clearly lacked the potency to stimulate significant DNA synthesis of urothelial cells in vitro.

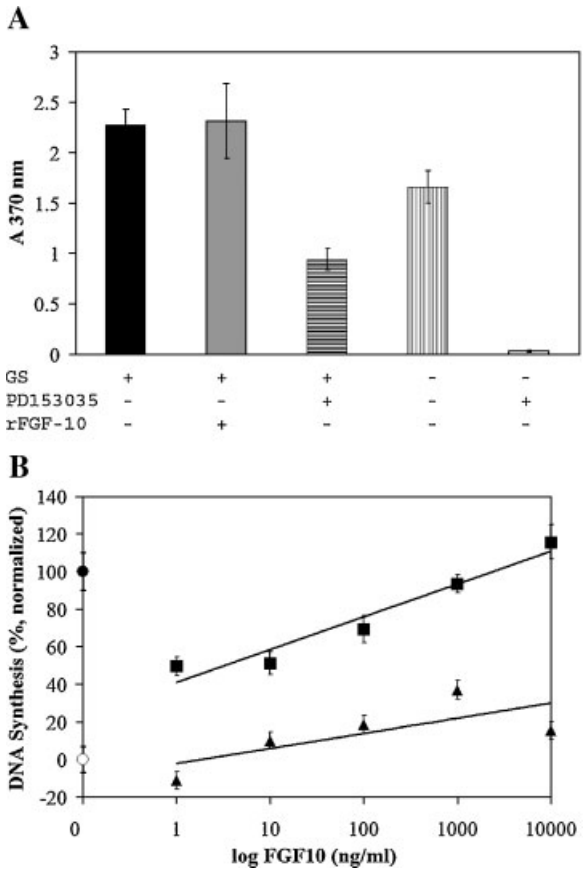

Fig. 5. Disruption of the NLS-like motif of FGF-10 negates mitogenic activity. **A**: Inhibition of growth factor-signaling pathways imposes cellular quiescence. Cells were grown in DKSFM medium containing 5 μg/ml heparin with and without growth supplement (GS), 1 μM EGFR inhibitor PD153035 (PD), and 1,000 ng/ml rFGF-10 (rFGF-10). DNA synthesis was measured by incorporation of a thymidine analog, BrdU, which was detected by immunocolorimetric methods at $A_{370\ nm}$. Error bars are standard error; n = 8. **B**: Induction of DNA synthesis in quiescent cells by rFGF-10 and rFGF-10(no NLS). Urothelial cells were grown as proliferating cells (closed circle) or as quiescent cells (open circle). Quiescent cells were exposed to increasing concentrations of rFGF-10 (squares) or rFGF-10(no NLS) (triangles). DNA synthesis assay and error calculation were performed as for panel A. All cells were grown in the presence of PD153035. n = 8.

Intracellular Localization of FGFR

The impotence of rFGF-10(no NLS) highlights the question of whether FGF-10 is acting independently or in concert with a partner inside the cell. Based on size, rFGF-10 should be able to diffuse into nuclei even without an NLS, whereas its receptor should require aid for nuclear entry. Immunofluorescence was used to reveal the intracellular distribution of the FGF-10 receptor in response to FGF-10 ligand. The

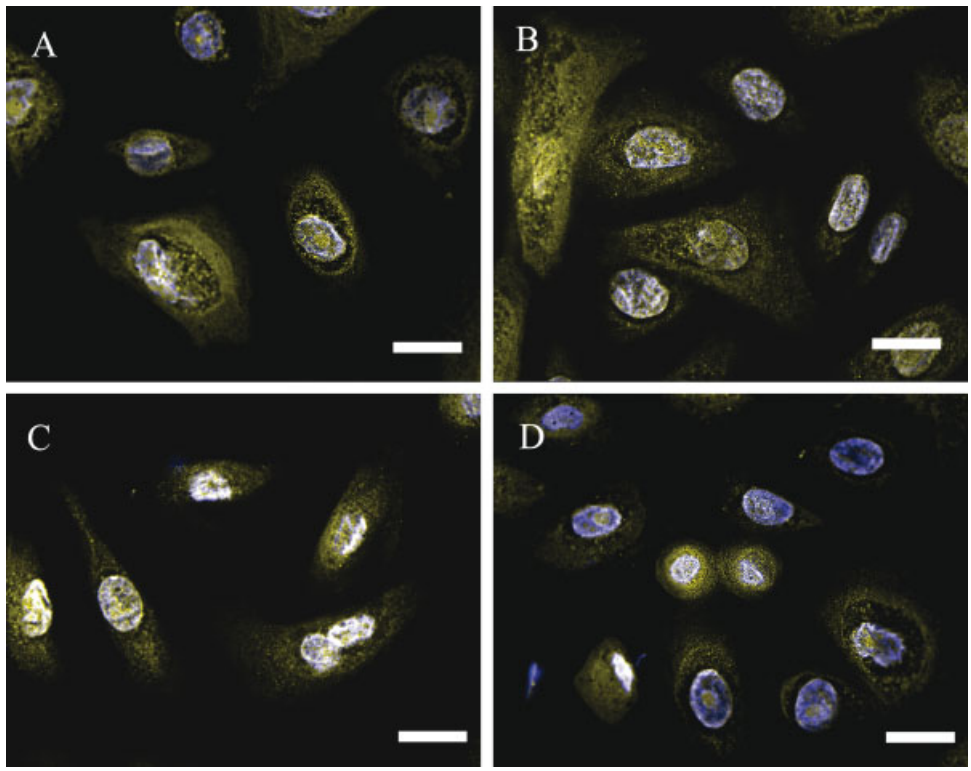

Fig. 6. Localization of FGF-10 receptor. Shown are merged optical slices of cultured urothelial cells stained for cell nuclei (blue) and the FGF-10 receptor (yellow). Co-localization of signals appears white. Slices were captured, deconvolved, and processed as in Figure 4, and represent a 0.3 μm thick cross-section through the cells. Cells were exposed to varying concentrations of rFGF-10 for 24 h. **A**: 0.0 μg/ml rFGF-10; (**B**) 0.5 μg/ml rFGF-10; (**C**) 5.0 μg/ml rFGF-10; (**D**) 50 μg/ml rFGF-10. Size bars = 20 μm.

FGF-10 receptor displayed the same staining pattern in cultured urothelial cells both in the absence (Fig. 6A) and presence (Fig. 6B–D) of saturating concentrations of rFGF-10 [Bottaro et al., 1990; Igarashi et al., 1998]. In optical slices, which greatly reduced ambiguity regarding intracellular localization, the FGF-10 receptor was observed at the cell periphery, in the cytoplasm, and in nuclei regardless of the concentration of rFGF-10. The FGF-10 receptor is noted for its specificity in the binding of ligands, and while it is known to bind FGFs other than FGF-10, including FGF-1, FGF-3, and FGF-7 [Bottaro et al., 1990; Aaronson et al., 1991; Luo et al., 1998], none of these growth factors were present. Normal urothelial cells do not synthesize their own FGFs as part of an autocrine stimulatory loop, although some transformed and cancerous cell lines have been known to do so [Jouanneau et al., 1991; Billottet et al., 2002]. Moreover, the experiment was performed in GS-free defined medium. Cells were washed extensively with this GS-free medium for a period of 24 h prior to starting this experiment to remove residual components of previous media. Therefore, the distribution of the FGF-10 receptor did not appear to be sensitive to the presence of ligand, although it could have returned to its initial equilibrium during the time course of the experiment. The signal for the FGF-10 receptor was most often punctate in the cytoplasm, which was consistent with previous descriptions of the transport of the receptor in clathrin-coated pits [Marchese et al., 1998], endosomes [Belleudi et al., 2002], and immunoreactive clusters [Zhang et al., 2006].

Co-localization of rFGF-10 and rFGF-10(no NLS) With FGFR

Having visualized separately the intracellular localization of rFGF-10, rFGF-10(no NLS), and the FGF-10 receptor, we sought to visualize the co-localization of these components to elucidate their relationship during intracellular transport. Cultured urothelial cells were exposed to rFGF-10 or rFGF-10(no NLS) for 47 h, fixed, and triple stained as described in

Materials and Methods Section. As in the preceding localization experiments, cells were subjected to optical sectioning by deconvolving stacks of images into a three-dimensional dataset. The optical sectioning was intended to eliminate ambiguity regarding whether a signal originated from above, below, or inside the nucleus. As already seen in Figure 4, rFGF-10 localized almost exclusively to cell nuclei (Fig. 7B), while rFGF-10(no NLS) was found both in cell nuclei and in the surrounding cytoplasm (Fig. 7H). This disparity reiterated that the loss of the NLS-like motif neither prevented rFGF-10(no NLS) from entering the cell, nor from entering the nucleus, but did dampen the nuclear localization effect. In Figure 7, panels C and I show the FGF-10 receptor both in cell nuclei and in cytoplasm, similar to results shown in Figure 6. This pattern of localization did not change whether the FGF-10 receptor was exposed to rFGF-10 or rFGF-10(no NLS). The merged images of rFGF-10 or rFGF-10(no NLS) with the FGF-10 receptor are shown in Figure 7D, J, respectively. While the co-localization of rFGF-10 with the FGF-10 receptor was confined largely to the nuclei, the signals of rFGF-10(no NLS) and the FGF-10 receptor appear to overlap throughout

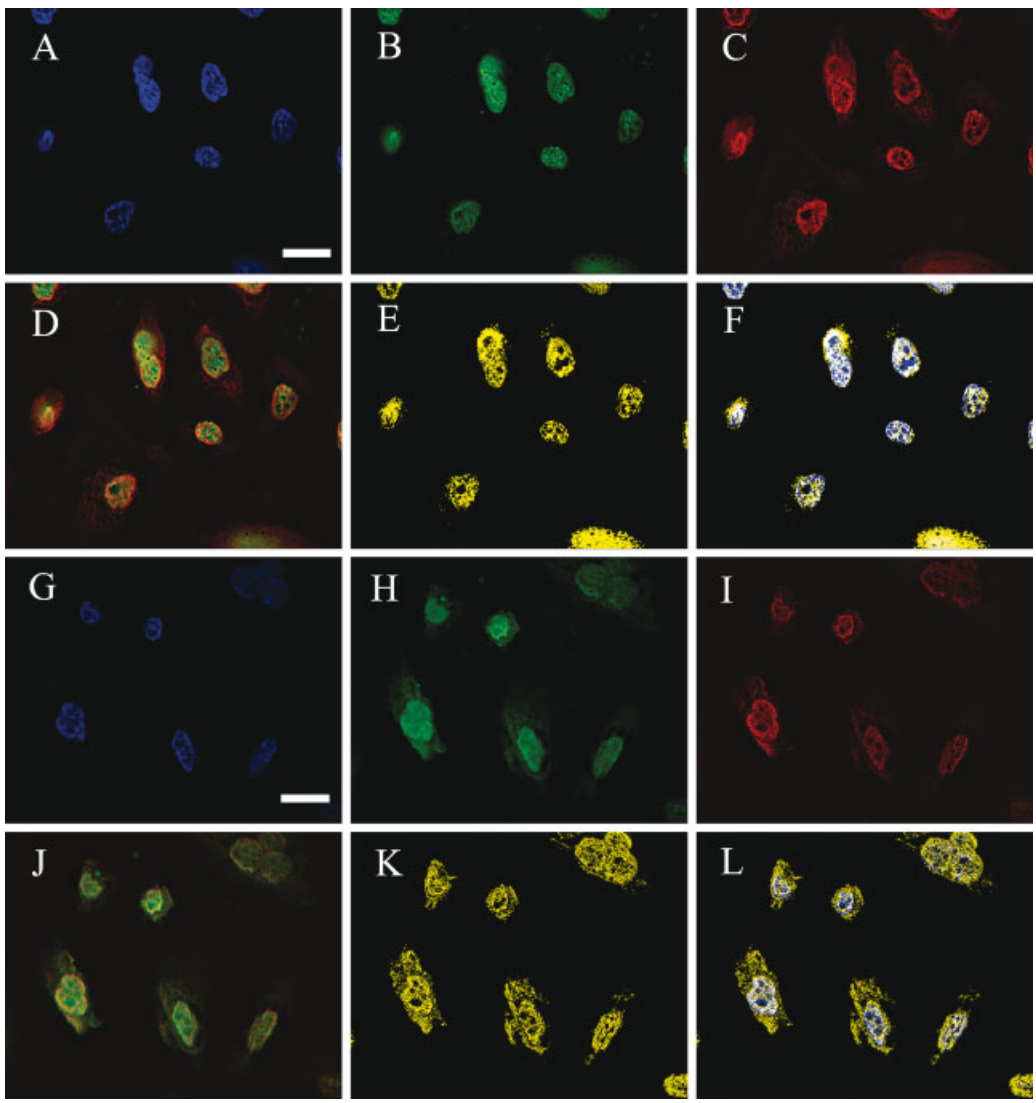

Fig. 7. Co-localization of rFGF-10 and rFGF-10(no NLS) with the FGF-10 receptor. Shown are optical slices 0.3 μm thick of cultured urothelial cells incubated with rFGF-10 or rFGF-10(no NLS). **A**: Cell nuclei stained with DAPI (blue); (**B**) cells stained for rFGF-10 (green); (**C**) cells stained for the FGF-10 receptor (red); (**D**) merge of panels B and C; (E) Co-localization of signals in panel D (shown in yellow); and (**F**) Merge of panels E and A. **Panels G–L** are the same as for **A–F**, respectively, except that rFGF-10(no NLS) was used in place of rFGF-10. Size bars = 20 μm.

TABLE I. Co-localization of rFGF-10 Proteins With Cell Nuclei and With the FGF-10 Receptor

	Localization in nuclei		Co-localization with FGFR		Co-localization with FGFR in nuclei	
	R_P	M (%)	R_P	M (%)	R_P	M (%)
rFGF10	0.84	92	0.77	95	0.69	89
rFGF10(no NLS)	0.76	60	0.79	69	0.51	61

The extent of co-localization of rFGF-10 and rFGF-10(no NLS) with cell nuclei and with the FGF-10 receptor was calculated using the immunofluorescence images in Figure 7.
R_P, Pearson's co-localization coefficient (scale −1 to +1); M, Manders' colocalization coefficient (range 0–100%).

the cells. These relationships were brought into greater clarity by isolating and displaying co-localized signals in yellow and excluding all independent signals (Fig. 7E,K). Finally, these co-localized signals in panels E and K were superimposed back upon the nuclear DAPI stain in panels A and G to clarify the observation that the co-localization of ligand and receptor occurred predominantly in nuclei for rFGF-10, but in both nuclei and cytoplasm for rFGF-10(no NLS).

The co-localization between two given sets of signals was quantified by calculating Pearson's co-localization coefficients (R_P) and Manders' co-localization coefficients (M) (Table I). R_P reflects a global co-localization correlation between two signals, whereas M relates the percent of one signal that co-localizes with another. Both rFGF-10 and rFGF-10(no NLS) displayed a positive co-localization to nuclei, although a far greater fraction of rFGF-10 was localized in nuclei than was rFGF-10(no NLS). Both growth factor variants also displayed a positive co-localization with the FGF-10 receptor. This association was particularly strong for rFGF-10, for a very high fraction of its total signal was found to co-localize with the receptor. rFGF-10(no NLS) associated with the FGF-10 receptor throughout the cytoplasm and nucleus, boosting its overall co-localization score. However, a relatively smaller fraction of its total signal was found to co-localize with the receptor. Finally, both growth factor–receptor complexes were found to localize to cell nuclei. A far greater fraction of these complexes were found in nuclei when constituted with rFGF-10 than with rFGF-10(no NLS).

DISCUSSION

The evidence that rFGF-10 is imported into urothelial cell nuclei is visually compelling. These cells are incapable of synthesizing their own FGF-10 and were supplied rFGF-10 only in the cell culture medium, yet the protein was clearly identified inside cell nuclei by deconvolution microscopy. Because rFGF-10 is a 20 kDa protein, it is small enough to diffuse into nuclei through nuclear pores. However, by the same token, rFGF-10 is also small enough to diffuse out of nuclei, so it should not accumulate there against any concentration gradient. A priori, the steady state equilibrium would be expected to be distributed between cytoplasm and nucleoplasm. Yet, the localization of rFGF-10 in the nucleus is far greater than can be accounted for by simple diffusion. Therefore, we postulate three additional explanations to account for the nuclear accumulation of rFGF-10.

First, intracellular rFGF-10 is constitutively imported into the nucleus via an NLS. An NLS might be sufficient to tip the equilibrium such that almost all of the rFGF-10 would be found in the nucleus. Indeed, just such a motif conforming to the consensus rules of an NLS was identified in FGF-10. A homologous motif found in FGF-1 was identified as an NLS and was able to drive the nuclear import of β-galactosidase [Zhan et al., 1992] and synthetic peptides [Lin et al., 1996] when appended to them. NLS-driven nuclear import was supported by the evidence gathered from observations of the rFGF-10(no NLS) mutant. This protein variant was minimally altered specifically to negate NLS-driven nuclear import. The disruption caused a markedly different staining pattern in urothelial cells, such that rFGF-10(no NLS) was diffusely present in cytoplasm to a far greater degree than the wild-type protein. Also, co-localization data confirmed that rFGF-10(no NLS) was less likely to reside in the nucleus than rFGF-10. However, despite the presence of rFGF-10(no NLS) in the cytoplasm, a significant fraction of the protein congregated in the

nucleus. It is possible that FGF-10 contains multiple NLS motifs, and that we have achieved only a partial disruption of nuclear localization activity, leaving an unknown number of NLS sites to be discovered.

In the NLS-dependent nuclear import of substrates from the cytoplasm, four factors thus far have been shown to be involved: importin-α, importin-β, RanGTP (nucleus), and RanGDP (cytoplasm). The NLS-containing cargo is bound in the cytoplasm by a heterodimeric import receptor that comprises importin-α and importin-β. Once inside the nucleus, an energy-dependent mechanism results in the release of the NLS-protein into the nucleoplasm and the recycling of importins back to the cytoplasm [Lange et al., 2007]. However the extent to which importins are present in urothelial cells and the degree of their interactions with rFGF-10 are currently unknown. Future experiments to determine the co-localization of rFGF-10 and importins are essential to definitively conclude that the putative NLS is a functional NLS. These experiments will bridge the gap in the literature concerning the function of importins in transitional urothelia and primary cultures of urothelial cells.

While it appears that the NLS-like motif of FGF-10 is a contributing factor to its nuclear localization, it is obvious that there are other, more dominant, forces driving this phenomenon.

We acknowledge that the disruption of the NLS-like motif may have unintentionally interfered with the three-dimensional structure of the protein. Alterations in the primary sequence of a protein, even the minimal alterations that created rFGF-10(no NLS), always pose the risk of interfering with protein folding. We evaluated the tertiary structures of rFGF-10 and rFGF-10(no NLS) by their intrinsic UV fluorescence emission spectra. The wavelength of maximum fluorescence of rFGF-10 (341.5 ± 0.5 nm) is more red-shifted than is often found in folded proteins. The fluorescence emission spectrum of a protein reflects the average environments of its tryptophan residues in terms of exposure to solvent. These environments are defined broadly in terms of three classes: class I is characterized as a buried, non-polar environment (λ_{max} 330–332 nm), class II is characterized as surface but limited solvent exposure (λ_{max} 340–342 nm), and class III is characterized as solvent exposed (λ_{max} 350–352 nm) [Davidson et al., 1999]. Tryptophans are usually found sheltered in the interior folds of proteins and display a fluorescence λ_{max} between class I and class II. The λ_{max} of rFGF-10 falls squarely into the class II category, implying that either the tryptophans are surface exposed or that the structure of the protein is flexible or unstable. Indeed, the crystal structure of FGF-10, captured in a complex with the FGF-10 receptor, shows both W41 and W131 on the surface of the protein (Fig. 1A) [Yeh et al., 2003], consistent with limited solvent exposure. The λ_{max} of rFGF-10(no NLS) (336.5 ± 0.5 nm) is shifted from that of the wild-type protein, raising the possibility that this mutant is misfolded, rather than minimally altered in the NLS region. However, three important facts argue against this possibility. First, the mutant is blue-shifted with regard to the wild-type, not red-shifted as would be the case with a destabilized protein. Second, the crystal structure shows that W131 is very close to the mutated NLS-like motif (Fig. 1A), within 3–5 angstroms of K98, and would be disproportionately influenced by any changes in this region. It is plausible that the change from electrically positive to electrically neutral residues in the NLS-like motif would produce a local change in environment responsible for shifting the fluorescence spectrum, and accounting for the differences between rFGF-10 and rFGF-10(no NLS). Third, the rFGF-10(no NLS) mutant does express in fermentation cultures and does possess unmistakable, if weak, biological activity.

A second contribution to the nuclear accumulation of rFGF-10 is that rFGF-10 is bound to the FGF-10 receptor inside the nucleus. The combined weight of these two molecules is far greater than 40 kDa, and is sufficient to prevent rFGF-10 diffusion back out of the nucleus. This attractive hypothesis would require rFGF-10 to exhibit strong binding to the FGF-10 receptor, a conclusion which is supported by the extensive co-localization of rFGF-10 with the FGF-10 receptor both inside the nucleus and throughout the cell. Furthermore, rFGF-10 bound to the FGF-10 receptor in the nucleus no longer factors into the steady-state equilibrium, but constitutes a pool of trapped protein. This pool enhances the concentration of rFGF-10 in the nucleus, in addition to that which enters by diffusion and via any NLS import. This reasoning also helps to account for the presence of rFGF-10(no NLS)

in the nucleus, for the growth factor variant was found to be mostly co-localized with its receptor in the nucleus. The changes in the NLS-like motif did not inhibit the ability of rFGF-10(no NLS) to bind its receptor, as revealed by the co-localization data, although they did disrupt its mitogenic activity. The nuclear import of the FGF-10-receptor complex may be even more efficient than that of rFGF-10 alone, for each has a putative NLS to contribute to the process. Indeed, the FGF-10 receptor itself has a potential NLS fitting the consensus definition of a bipartite sequence [Dingwall and Laskey, 1991] which spans residues 406–422 [Dell and Williams, 1992]. This new identification of an NLS in the FGF-10 receptor helps explain its observed intracellular distribution. A closely related receptor, FGFR-1, has already been shown to be translocated into cell nuclei via interactions between importins and its NLS [Reilly and Maher, 2001]. While the translocation of this complex through the cytoplasm was not clearly observed in these or previous experiments [Zhang et al., 2006], it has been supported by other reports [Marchese et al., 1998; Belleudi et al., 2002]. The presence, strength, and effect of an NLS in the FGF-10 transmembrane receptor merits consideration in future studies.

A third explanation for the observed accumulation of nuclear rFGF-10 is that it binds directly or indirectly to some other component of the nucleus and is prevented from diffusing out. The crowded nuclear milieu can enhance association constants [Hancock, 2004], and may allow rFGF-10 to find a binding partner. Given the precipitous drop in the mitogenic activity of rFGF-10(no NLS), it is an enticing possibility that a link to the transcriptional machinery occurs at or near this motif. The failure to make such a connection would explain why the NLS-like motif of FGF-10 is essential for mitogenesis. While the mechanism of the mitogenic activity of rFGF-10 inside the nucleus is a matter of speculation, there are enlightening precedents. In concert with its receptor FGFR-1, nuclear FGF-2 is able to activate c-Jun and induce expression of cyclin D [Reilly and Maher, 2001]. The FGF-10 receptor alone also has tantalizing possible functions in the nucleus. Nuclear FGFR-1 is enriched in the nuclear matrix fraction of proliferating cells, but not of quiescent cells [Maher, 1996]. Nuclear EGF receptor is able to both bind transcription factors and act as one itself, activating transcription at specific promoter regions of DNA that result in cell proliferation [Lin et al., 2001; Lo et al., 2005]. These recently discovered activities offer a rationale for the transport of extracellular growth factors and transmembrane receptors to the nucleus that is complementary to and a logical extension of the growth factors' known mitogenic signaling activity.

Regardless of the mechanism of transport, this new information continues to strengthen FGF-10's potential therapeutic value in urinary tract repair. It has already been noted that FGF-10 stimulates only urothelial cell proliferation, not that of smooth muscle or fibroblast cells [Zhang et al., 2006]. Other proteins, such as FGF-binding protein, are also known to be upregulated during times of injury to epithelial tissue, and enhance the proliferative effect of low concentrations of FGF-10 [Beer et al., 2005]. Thus, if rFGF-10 were administered into the lumen of the bladder, it would have a specific target and would stimulate the proliferation and repair of the urothelium. Here, we show that FGF-10 also stimulates only quiescent urothelial cell mitogenesis, and does not augment cells already proliferating (Fig. 5A), which would help ensure that cell growth does not expand out of control. There is also good reason to believe that if eliminating the NLS-like motif of FGF-10 cripples its mitogenic effect, then other alterations may create an even more potent growth factor. Given the exponential growth of cells, even a small boost to the proliferative rate of urothelial cells would have a significant effect on cell number within days, promoting rapid regeneration and healing.

ACKNOWLEDGMENTS

We thank Dr. Richard Grady and Dr. Byron Joyner for the collection of urothelial tissue and Kristy Seidel for assistance with statistical analysis. This study was supported by grants from the NIH (DK062251) to J.A. Bassuk and an NIDDK NRSA post-doctoral traineeship to J. Kosman through the Department of Urology, University of Washington.

REFERENCES

Aaronson SA, Bottaro DP, Miki T, Ron D, Finch PW, Fleming TP, Ahn J, Taylor WG, Rubin JS. 1991. Keratinocyte growth factor. A fibroblast growth factor

family member with unusual target cell specificity. Ann N Y Acad Sci 638:62–77.
Bagai S, Rubio E, Cheng JF, Sweet R, Thomas R, Fuchs E, Grady R, Mitchell M, Bassuk JA. 2002. Fibroblast growth factor-10 is a mitogen for urothelial cells. J Biol Chem 277:23828–23837.
Beer HD, Bittner M, Niklaus G, Munding C, Max N, Goppelt A, Werner S. 2005. The fibroblast growth factor binding protein is a novel interaction partner of FGF-7, FGF-10 and FGF-22 and regulates FGF activity: Implications for epithelial repair. Oncogene 24:5269–5277.
Belleudi F, Ceridono M, Capone A, Serafino A, Marchese C, Picardo M, Frati L, Torrisi MR. 2002. The endocytic pathway followed by the keratinocyte growth factor receptor. Histochem Cell Biol 118:1–10.
Billottet C, Janji B, Thiery JP, Jouanneau J. 2002. Rapid tumor development and potent vascularization are independent events in carcinoma producing FGF-1 or FGF-2. Oncogene 21:8128–8139.
Bottaro DP, Rubin JS, Ron D, Finch PW, Florio C, Aaronson SA. 1990. Characterization of the receptor for keratinocyte growth factor. Evidence for multiple fibroblast growth factor receptors. J Biol Chem 265:12767–12770.
Boulikas T. 1993. Nuclear localization signals (NLS). Crit Rev Eukaryot Gene Expr 3:193–227.
Claus P, Doring F, Gringel S, Muller-Ostermeyer F, Fuhlrott J, Kraft T, Grothe C. 2003. Differential intranuclear localization of fibroblast growth factor-2 isoforms and specific interaction with the survival of motoneuron protein. J Biol Chem 278:479–485.
Cokol M, Nair R, Rost B. 2000. Finding nuclear localization signals. EMBO Rep 1:411–415.
Davidson WS, Arnvig-McGuire K, Kennedy A, Kosman J, Hazlett TL, Jonas A. 1999. Structural organization of the N-terminal domain of apolipoprotein A-I: Studies of tryptophan mutants. Biochemistry 38: 14387–14395.
Dell KR, Williams LT. 1992. A novel form of fibroblast growth factor receptor 2. Alternative splicing of the third immunoglobulin-like domain confers ligand binding specificity. J Biol Chem 267:21225–21229.
Dingwall C, Laskey RA. 1991. Nuclear targeting sequences—a consensus? Trends Biochem Sci 16:478–481.
Freeman MR, Yoo JJ, Raab G, Soker S, Adam RM, Schneck FX, Renshaw AA, Klagsbrun M, Atala A. 1997. Heparin-binding EGF-like growth factor is an autocrine growth factor for human urothelial cells and is synthesized by epithelial and smooth muscle cells in the human bladder. J Clin Invest 99:1028–1036.
Fry DW, Kraker AJ, McMichael A, Ambroso LA, Nelson JM, Leopold WR, Connors RW, Bridges AJ. 1994. A specific inhibitor of the epidermal growth factor receptor tyrosine kinase. Science 265:1093–1095.
Hainau B, Dombernowsky P. 1974. Histology and cell proliferation in human bladder tumors. An autoradiographic study. Cancer 33:115–126.
Hancock R. 2004. Internal organisation of the nucleus: Assembly of compartments by macromolecular crowding and the nuclear matrix model. Biol Cell 96:595–601.
Hicks RM. 1975. The mammalian urinary bladder: An accommodating organ. Biol Rev Camb Philos Soc 50:215–246.
Igarashi M, Finch PW, Aaronson SA. 1998. Characterization of recombinant human fibroblast growth factor (FGF)-10 reveals functional similarities with keratinocyte growth factor (FGF-7). J Biol Chem 273:13230–13235.
Imamura T, Tokita Y, Mitsui Y. 1992. Identification of a heparin-binding growth factor-1 nuclear translocation sequence by deletion mutation analysis. J Biol Chem 267: 5676–5679.
Jouanneau J, Gavrilovic J, Caruelle D, Jaye M, Moens G, Caruelle JP, Thiery JP. 1991. Secreted or nonsecreted forms of acidic fibroblast growth factor produced by transfected epithelial cells influence cell morphology, motility, and invasive potential. Proc Natl Acad Sci USA 88:2893–2897.
Kalderon D, Richardson WD, Markham AF, Smith AE. 1984a. Sequence requirements for nuclear location of simian virus 40 large-T antigen. Nature 311:33–38.
Kalderon D, Roberts BL, Richardson WD, Smith AE. 1984b. A short amino acid sequence able to specify nuclear location. Cell 39:499–509.
Kiefer P, Dickson C. 1995. Nucleolar association of fibroblast growth factor 3 via specific sequence motifs has inhibitory effects on cell growth. Mol Cell Biol 15: 4364–4374.
Kiefer P, Acland P, Pappin D, Peters G, Dickson C. 1994. Competition between nuclear localization and secretory signals determines the subcellular fate of a single CUG-initiated form of FGF3. EMBO J 13:4126–4136.
Lange A, Mills RE, Lange CJ, Stewart M, Devine SE, Corbett AH. 2007. Classical nuclear localization signals: Definition, function, and interaction with importin alpha. J Biol Chem 282: 5101–5105.
Lin YZ, Yao SY, Hawiger J. 1996. Role of the nuclear localization sequence in fibroblast growth factor-1-stimulated mitogenic pathways. J Biol Chem 271: 5305–5308.
Lin SY, Makino K, Xia W, Matin A, Wen Y, Kwong KY, Bourguignon L, Hung MC. 2001. Nuclear localization of EGF receptor and its potential new role as a transcription factor. Nat Cell Biol 3:802–808.
Lo HW, Hsu SC, Ali-Seyed M, Gunduz M, Xia W, Wei Y, Bartholomeusz G, Shih JY, Hung MC. 2005. Nuclear interaction of EGFR and STAT3 in the activation of the iNOS/NO pathway. Cancer Cell 7:575–589.
Lu W, Luo Y, Kan M, McKeehan WL. 1999. Fibroblast growth factor-10. A second candidate stromal to epithelial cell andromedin in prostate. J Biol Chem 274:12827–12834.
Luo Y, Lu W, Mohamedali KA, Jang JH, Jones RB, Gabriel JL, Kan M, McKeehan WL. 1998. The glycine box: A determinant of specificity for fibroblast growth factor. Biochemistry 37:16506–16515.
Luo Y, Cho HH, Jones RB, Jin C, McKeehan WL. 2004. Improved production of recombinant fibroblast growth factor 7 (FGF7/KGF) from bacteria in high magnesium chloride. Protein Expr Purif 33:326–331.
Maher PA. 1996. Nuclear Translocation of fibroblast growth factor (FGF) receptors in response to FGF-2. J Cell Biol 134:529–536.
Manders EM, Stap J, Brakenhoff GJ, van Driel R, Aten JA. 1992. Dynamics of three-dimensional replication patterns during the S-phase, analysed by double labelling of DNA and confocal microscopy. J Cell Sci 103:857–862.

Marceau N. 1990. Cell lineages and differentiation programs in epidermal, urothelial and hepatic tissues and their neoplasms. Lab Invest 63:4–20.

Marchese C, Mancini P, Belleudi F, Felici A, Gradini R, Sansolini T, Frati L, Torrisi MR. 1998. Receptor-mediated endocytosis of keratinocyte growth factor. J Cell Sci 111:3517–3527.

Min H, Danilenko DM, Scully SA, Bolon B, Ring BD, Tarpley JE, DeRose M, Simonet WS. 1998. Fgf-10 is required for both limb and lung development and exhibits striking functional similarity to Drosophila branchless. Genes Dev 12:3156–3161.

Nakai K, Horton P. 1999. PSORT: a program for detecting sorting signals in proteins and predicting their subcellular localization. Trends Biochem Sci 24:34–36.

Nishimura T, Nakatake Y, Konishi M, Itoh N. 2000. Identification of a novel FGF, FGF-21, preferentially expressed in the liver. Biochim Biophys Acta 1492:203–206.

Picard D, Yamamoto KR. 1987. Two signals mediate hormone-dependent nuclear localization of the glucocorticoid receptor. EMBO J 6:3333–3340.

Quarto N, Finger FP, Rifkin DB. 1991. The NH2-terminal extension of high molecular weight bFGF is a nuclear targeting signal. J Cell Physiol 147:311–318.

Rebel JM, De Boer WI, Thijssen CD, Vermey M, Zwarthoff EC, Van der Kwast TH. 1994. An in vitro model of urothelial regeneration: effects of growth factors and extracellular matrix proteins. J Pathol 173:283–291.

Reilly JF, Maher PA. 2001. Importin beta-mediated nuclear import of fibroblast growth factor receptor: role in cell proliferation. J Cell Biol 152:1307–1312.

Robbins J, Dilworth SM, Laskey RA, Dingwall C. 1991. Two interdependent basic domains in nucleoplasmin nuclear targeting sequence: Identification of a class of bipartite nuclear targeting sequence. Cell 64:615–623.

Sheng Z, Lewis JA, Chirico WJ. 2004. Nuclear and nucleolar localization of 18-kDa fibroblast growth factor-2 is controlled by C-terminal signals. J Biol Chem 279:40153–40160.

Silver PA. 1991. How proteins enter the nucleus. Cell 64: 489–497.

Stachowiak MK, Moffett J, Maher P, Tucholski J, Stachowiak EK. 1997. Growth factor regulation of cell growth and proliferation in the nervous system. A new intracrine nuclear mechanism. Mol Neurobiol 15:257–283.

Stewart FA. 1986. Mechanism of bladder damage and repair after treatment with radiation and cytostatic drugs. Br J Cancer (Suppl 7):280–291.

Truant R, Fridell RA, Benson RE, Bogerd H, Cullen BR. 1998. Identification and functional characterization of a novel nuclear localization signal present in the yeast Nab2 poly(A)+ RNA binding protein. Mol Cell Biol 18:1449–1458.

Varley CL, Stahlschmidt J, Lee WC, Holder J, Diggle C, Selby PJ, Trejdosiewicz LK, Southgate J. 2004. Role of PPARgamma and EGFR signalling in the urothelial terminal differentiation programme. J Cell Sci 117: 2029–2036.

Varley C, Hill G, Pellegrin S, Shaw NJ, Selby PJ, Trejdosiewicz LK, Southgate J. 2005. Autocrine regulation of human urothelial cell proliferation and migration during regenerative responses in vitro. Exp Cell Res 306: 216–229.

Yeh BK, Igarashi M, Eliseenkova AV, Plotnikov AN, Sher I, Ron D, Aaronson SA, Mohammadi M. 2003. Structural basis by which alternative splicing confers specificity in fibroblast growth factor receptors. Proc Natl Acad Sci USA 100:2266–2271.

Yucel S, Liu W, Cordero D, Donjacour A, Cunha G, Baskin LS. 2004. Anatomical studies of the fibroblast growth factor-10 mutant, Sonic Hedge Hog mutant and androgen receptor mutant mouse genital tubercle. Adv Exp Med Biol 545:123–148.

Zhan X, Hu X, Friedman S, Maciag T. 1992. Analysis of endogenous and exogenous nuclear translocation of fibroblast growth factor-1 in NIH 3T3 cells. Biochem Biophys Res Commun 188:982–991.

Zhang D, Kosman J, Carmean N, Grady R, Bassuk JA. 2006. FGF-10 and its receptor exhibit bidirectional paracrine targeting to urothelial and smooth muscle cells in the lower urinary tract. Am J Physiol Renal Physiol 291:F481–F494.